

MoE-ACT: Scaling Multi-Task Bimanual Manipulation with Sparse Language-Conditioned Mixture-of-Experts Transformers

Kangjun Guo, Haichao Liu, Yanji Sun, Ruhan Zhao, Jinni Zhou, Jun Ma, *Senior Member, IEEE*

Abstract—The ability of robots to handle multiple tasks under a unified policy is critical for deploying embodied intelligence in real-world household and industrial applications. However, out-of-distribution variation across tasks often causes severe task interference and negative transfer when training general robotic policies. To address this challenge, we propose a lightweight multi-task imitation learning framework for bimanual manipulation, termed Mixture-of-Experts-Enhanced Action Chunking Transformer (MoE-ACT), which integrates sparse Mixture-of-Experts (MoE) modules into the Transformer encoder of ACT. The MoE layer decomposes a unified task policy into independently invoked expert components. Through adaptive activation, it naturally decouples multi-task action distributions in latent space. During decoding, Feature-wise Linear Modulation (FiLM) dynamically modulates action tokens to improve consistency between action generation and task instructions. In parallel, multi-scale cross-attention enables the policy to simultaneously focus on both low-level and high-level semantic features, providing rich visual information for robotic manipulation. We further incorporate textual information, transitioning the framework from a purely vision-based model to a vision-centric, language-conditioned action generation system. Experimental validation in both simulation and a real-world dual-arm setup shows that MoE-ACT substantially improves multi-task performance. Specifically, MoE-ACT outperforms vanilla ACT by an average of 33% in success rate. These results indicate that MoE-ACT provides stronger robustness and generalization in complex multi-task bimanual manipulation environments. Our open-source project page can be found at <https://j3k7.github.io/MoE-ACT/>.

I. INTRODUCTION

Robotic manipulation is important in both industrial and household settings, where it can reduce human labor requirements. Existing research has primarily focused on single-task execution. Imitation and reinforcement learning methods, such as Diffusion Policy [1] and Action Chunking with Transformers (ACT) [2], have demonstrated high success rates and strong robustness in such settings. However, dynamic real-world environments require robots to perform multiple tasks within a unified model [3], [4]. Therefore, effective multi-task generalization is essential for broader practical deployment.

In robotic task learning, accurate modeling of action distributions is central to policy learning. Robotic manipulation is not a simple linear mapping from pixels to coordinates; rather, it requires modeling complex probability distributions

in high-dimensional continuous spaces. Diffusion policies have achieved strong performance on complex manipulation tasks by formulating action generation as a denoising process [5], [6]. ACT models action prediction in chunked sequences using a CVAE architecture, which effectively captures multimodal expert demonstrations and mitigates compounding errors in imitation learning. However, in multi-task settings, conflicts between task objectives and entanglement among action distributions often lead to severe “task entanglement” in the decision space [7], [8]. This increases the difficulty of modeling multi-horizon goals and degrades the effectiveness of straightforward imitation learning.

Large-scale Vision-Language-Action (VLA) models have emerged as a promising paradigm for general-purpose robotic policies [9]–[12]. Representative examples, such as π_0 [11] and RDT [12], typically contain billions of parameters. Pre-training on large multimodal datasets substantially improves zero-shot generalization and open-world task execution. However, this paradigm requires substantial computational resources and extensive training data. Moreover, due to their model scale, inference latency often fails to satisfy real-time robotic constraints [13]. Therefore, improving multi-task performance while maintaining model compactness and inference efficiency remains an important objective.

A promising architecture for this challenge is the MoE framework [14], [15]. MoE has been widely adopted in large language models [16], [17] and multi-task robotics [18]–[20]. It decomposes a model into specialized expert components, each focusing on different tasks or data characteristics. The model then selectively activates relevant experts based on the input, preserving computational efficiency.

In this work, we propose MoE-ACT for efficient multi-task dual-arm manipulation. We integrate the MoE module into the Transformer encoder. With a learnable routing mechanism, the model adaptively emphasizes task-relevant visual features, thereby decoupling task representations. We also introduce language embeddings to improve task identification. By combining sparse expert routing with multi-scale feature fusion, MoE-ACT addresses the performance limitations of single-policy approaches in complex scenarios and provides an efficient paradigm for building robust general robotic models.

In summary, the contributions of this paper are as follows:

- We propose MoE-ACT, a robotic manipulation policy designed for multi-task learning and efficient operation tailored for dual-arm robots.
- In the Transformer decoder, we integrate Feature-wise

Kangjun Guo, Haichao Liu, Yanji Sun, Ruhan Zhao, Jinni Zhou are with The Hong Kong University of Science and Technology (Guangzhou), Guangzhou 511453, China (e-mail: {kguo886, hliu369, ysun993, rzhao238}@connect.hkust-gz.edu.cn; eejinni@hkust-gz.edu.cn).

Jun Ma is with The Hong Kong University of Science and Technology (Guangzhou), Guangzhou 511453, China, and also with The Hong Kong University of Science and Technology, Hong Kong SAR, China (e-mail: jun.ma@ust.hk).

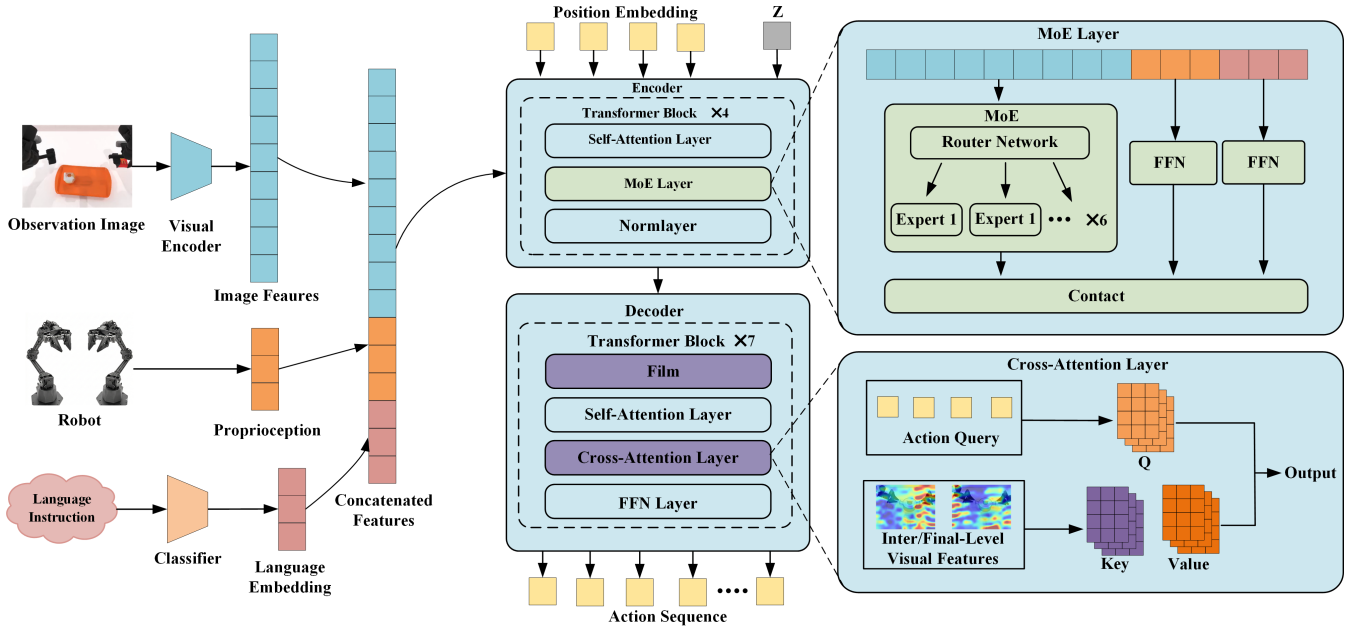


Fig. 1: Overview of MoE-ACT. The architecture consists of the MoE module integrated into the Transformer encoder and a FiLM mechanism in the decoder. The MoE module enables task-specific feature decoupling, while FiLM ensures that action generation is consistent with task instructions. Multi-scale cross-attention allows the model to capture both high-level semantics and low-level visual details for manipulation control.

Linear Modulation (FiLM) to dynamically adjust action tokens, ensuring high consistency between generated actions and task instructions.

- We introduce multi-scale cross-attention into the Transformer decoder to directly capture low-level visual details. This enables deeper fusion of environment perception and action generation, substantially improving performance in complex manipulation scenarios.
- The effectiveness of the proposed method is validated through both simulation and real-world experiments. These results prove that MoE has the capacity for task decomposition and highlight its effectiveness in handling multiple tasks.

II. RELATED WORKS

A. Imitation Learning for Robotic Manipulation

Recently, imitation learning has made significant progress in helping robots acquire complex manipulation skills [1], [2], [21]. This paradigm learns directly from expert demonstration data, allowing robots to efficiently capture complex trajectory distributions and establish a direct mapping from perception to action [22].

As a representative architecture in this field, the ACT policy [2] is trained via a CVAE and models the action prediction as action chunks to reduce compounding errors. Compared to diffusion policies, ACT provides faster inference as it avoids the time-consuming iterative denoising process. However, due to the lack of language modality input, the original ACT is unable to leverage semantic context to focus on task-relevant visual features. To address this issue, MT-ACT [23] introduces task language instructions to enhance the multi-task learning capabilities of ACT. Additionally, BAKU

[24], a simple transformer architecture built upon ACT, enables the efficient multi-task robot learning. Despite these advances, multi-task learning remains a significant challenge for imitation learning.

With the advancement of multimodal learning, VLA models have emerged as a mainstream paradigm for general-purpose robotic policies [25]. VLA models, such as Google’s RT-2 [9] and OpenVLA [10], integrate multi-modal perceptual capabilities of pre-trained Vision-Language Models (VLMs) with robotic action spaces, leveraging large-scale data training to comprehend complex environments. This enables robots to perform high-level reasoning and generalize across open-world tasks. However, the performance of large VLA models is heavily dependent on large-scale simulation and real-world embodied data. Furthermore, VLA models still face several challenges, such as high training costs, significant GPU memory consumption, and slow inference speeds [26].

To address these challenges, this work introduces a lightweight MoE-ACT that incorporates language instruction as a semantic guide. And MoE-ACT integrates the MoE mechanism into the Transformer encoder to decouple task representations and enhance multi-task performance.

B. Multi-task Learning in Robotics

Multi-task learning enables robots to perform varied tasks in diverse settings. Nowadays, significant advancements have been achieved in multi-task learning in robotic manipulation. Training on large-scale datasets, such as Open X-Embodiment [27] and DROID [28], can significantly enhance the generalization performance and multi-task capabilities of robot models in complex scenarios. For example, π_0 [11]

demonstrates superior performance in handling complex manipulation tasks through joint training on large-scale mixed robot datasets.

Many studies have advanced multi-task learning through innovations in policy architecture [8], [29]–[31]. For instance, skill-based policies significantly enhance model generalization by abstracting and reusing task-invariant skills across various tasks. Discrete Policy [8] employs VQ-VAE to abstract continuous action sequences into discrete latent skill identifiers. By integrating generative models within a decoupled latent space, this approach enables the reuse of various manipulation skills across different tasks. Similarly, SkillDiffuser [31] combines discrete skill representations with conditional diffusion models to map abstract instructions to consistent action sequences, significantly improving skill reuse and model generalization in multi-task scenarios.

The MoE architecture has shown strong potential for multi-task robotic learning. By enabling different subnetworks to specialize in distinct skills, MoE improves task decomposition and overall robustness. In robotic manipulation, MoE has been applied to improve diffusion policies [32]–[34]. For example, MoE-DP inserts an MoE layer between the vision encoder and the diffusion model, improving robustness to interference and long-horizon task execution [33]. MoE is also used to scale model capacity and regulate computational flow across diffusion-policy modules [34]. Since MoE is originally developed for Transformer architectures [16], the Transformer-based ACT provides a more natural foundation for its integration. Integrating MoE with ACT preserves high inference efficiency while offering substantial performance gains in multi-task settings.

III. METHODOLOGY

MoE-ACT is a unified framework designed for robotic multi-task manipulation. Fig. 1 shows the overview of MoE-ACT. The approach builds upon ACT [2]. The integration of the MoE mechanism within the Transformer encoder and a FiLM mechanism within the decoder can address the challenges of negative transfer and task interference in multi-task learning. Furthermore, an additional cross-attention layer is introduced in the decoder to enhance the model’s perception of low-level visual features.

A. Problem Formulation and Overview

This work considers a multi-task imitation learning setting in which a robot learns a policy π to perform N_{task} distinct tasks. At each time step t , the policy receives an observation \mathcal{O}_t consisting of joint positions $q_t \in \mathbb{R}^{d_a}$ and RGB images $I_t \in \mathbb{R}^{H \times W \times 3}$ from multiple camera views. A language instruction l is also provided. The objective is to predict a sequence of future actions $\mathbf{a}_{t:t+k}$, where k denotes the action chunk size. The overall MoE-ACT architecture contains three main components: (1) an MoE-enhanced encoder that processes visual and proprioceptive inputs and dynamically routes image tokens to specific experts to decouple feature representations; (2) a Transformer decoder that generates

actions conditioned on the task embedding via FiLM and attends to multi-scale features to improve manipulation performance; and (3) a CVAE encoder that maps action sequences into a latent space z to implicitly capture diverse behavioral modes in the data.

B. MoE-Enhanced Encoder

Standard Transformers process all inputs with shared parameters, which can cause conflicting gradient updates across diverse tasks. To mitigate this issue, we integrate an MoE module into the feed-forward networks (FFNs) of the Transformer encoder layers. The MoE module consists of a routing network and a collection of N expert networks (FFNs). The routing network dynamically computes the activation weight of each expert from the input features. We adopt a sample-level routing strategy in which all image tokens from the same observation frame are routed to the same expert subset, ensuring spatial consistency in feature processing. Let the input sequence to the l -th encoder layer be $X^l = [x_{cls}, x_{prop}, x_{task}, x_{img}^1, \dots, x_{img}^M]$. The gating input $G(\cdot)$ is constructed by concatenating proprioception, the task embedding, and the global average of image tokens:

$$h_{router_input} = \text{Concat} \left(x_{prop}, x_{task}, \frac{1}{M} \sum_{j=1}^M x_{img}^j \right) \quad (1)$$

The routing logits are computed as:

$$H(x) = W_g \cdot h_{router_input} + \epsilon, \quad \epsilon \sim \mathcal{N}(0, \sigma^2) \quad (2)$$

where $W_g \in \mathbb{R}^{E \times d_{model}}$ is a learnable weight matrix, E is the total number of experts, and ϵ is Gaussian noise added during training for exploration.

The router selectively activates the top- k experts with the highest logits. In this work, we set $k = 2$. The gating weights are obtained via Softmax over the selected experts:

$$P(e|x)_i = \begin{cases} \frac{\exp(H(x)_i)}{\sum_{j \in \text{Top-}k(H(x))} \exp(H(x)_j)} & \text{if } i \in \text{Top-}k(H(x)) \\ 0 & \text{otherwise} \end{cases} \quad (3)$$

The final MoE output is the probability-weighted sum of the activated expert outputs. This sparse activation mechanism substantially increases parameter capacity with negligible computational overhead, improving performance in complex multi-task scenarios. In our implementation, non-image tokens (e.g., x_{prop} and x_{task}) bypass the MoE module and are processed by a shared FFN to maintain stable control-signal representations. For image tokens x_{img} , the output is the weighted sum of selected experts:

$$\text{FFN}_{MoE}(x_{img}) = \sum_{i=1}^E P(e|x)_i \cdot E_i(x_{img}) \quad (4)$$

where $E_i(\cdot)$ represents the i -th expert network (a 2-layer MLP).

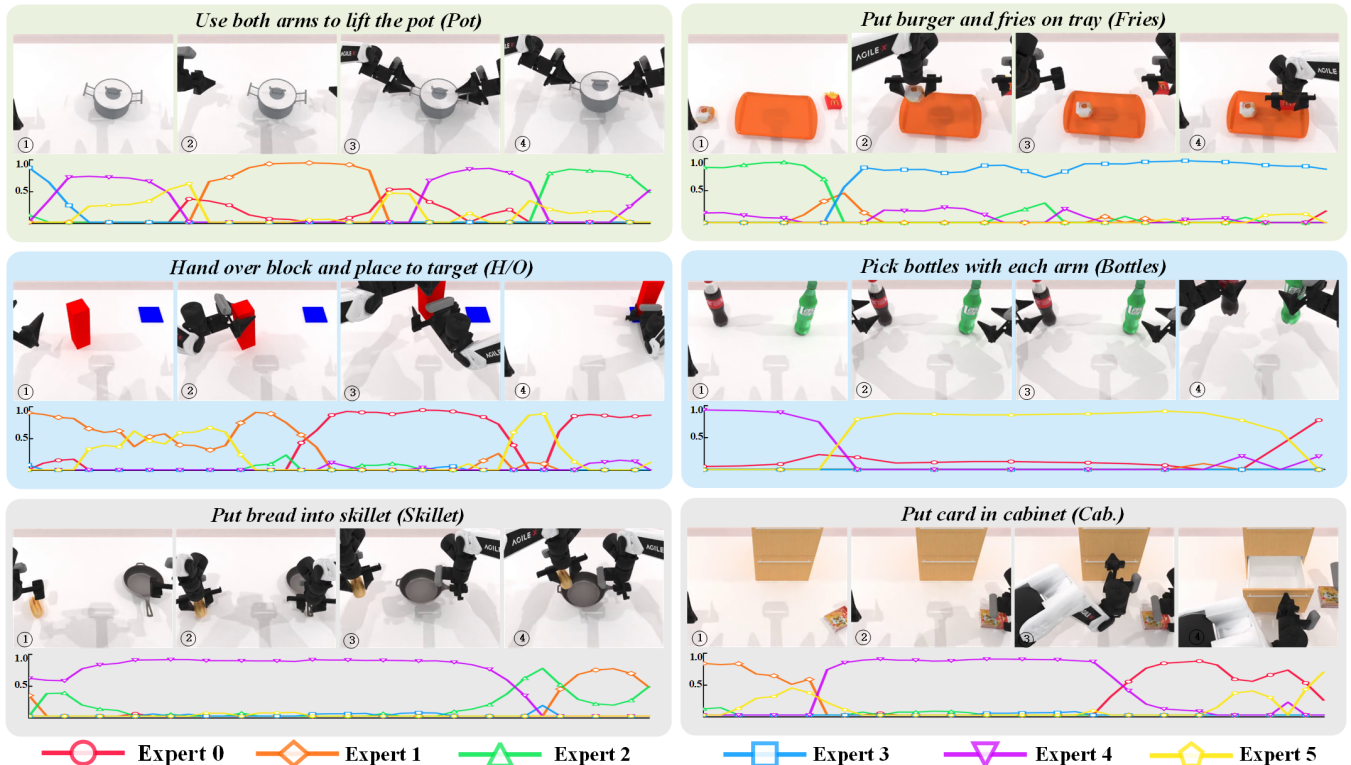


Fig. 2: Multi-task learning experiments in RoboTwin 2.0. MoE-ACT demonstrates superior performance across all six tasks, significantly outperforming the original ACT and other baselines. The line chart illustrates the evolution of selection weights for different experts over time.

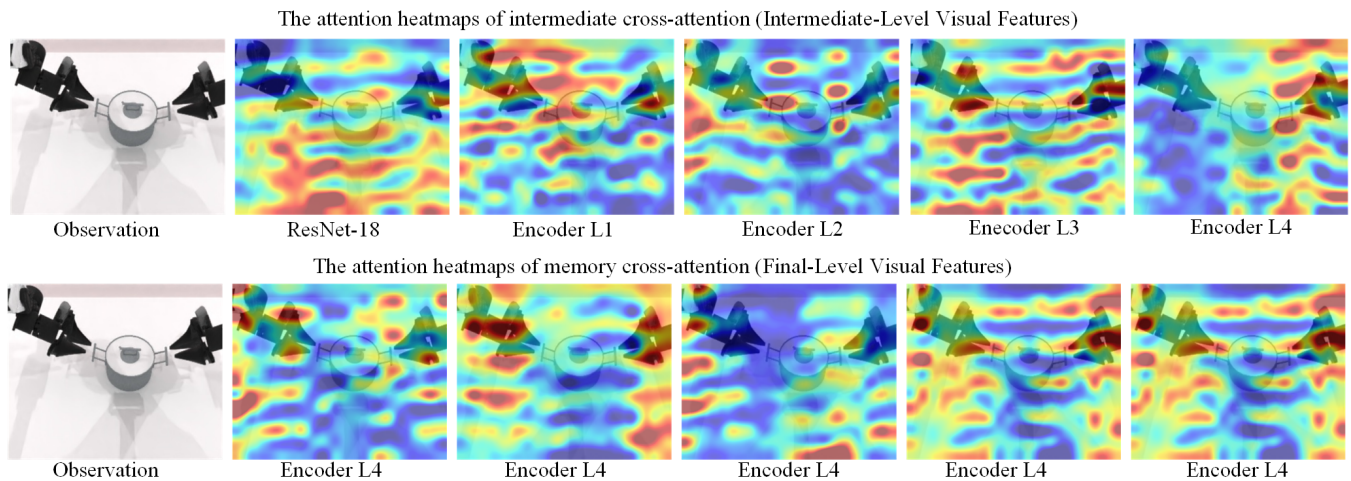


Fig. 3: Attention heatmap of MoE-ACT on RoboTwin 2.0. The top row displays attention on intermediate-level visual features, while the bottom row shows attention on final-level contextualized features across five decoder layers (L1-L5). The color intensity corresponds to the attention magnitude, where brighter regions indicate higher values.

C. Task-Conditioned Transformer Decoder

The decoder is responsible for translating the encoded features into precise action sequences. We enhance the standard Transformer decoder with two mechanisms: task conditioning via FiLM and multi-scale feature fusion.

1) *Task-conditioned FiLM*: To ensure that generated actions strictly follow task instructions, we apply task-conditioned FiLM at each decoder layer. The language instruction is first processed by a classifier to identify the task and assign a unique task embedding. The FiLM module then

TABLE I: Bimanual multi-task learning performance on RoboTwin 2.0

Methods	Bottle	H/O	Pot	Fries	Skillet	Cab.	Avg.
ACT [2]	42	4	59	10	4	15	22
DP [1]	23	29	10	5	3	43	19
RDT [12]	55	60	63	66	5	43	49
BAKU [24]	26	6	80	46	2	28	31
MoE-ACT (ours)	52	70	76	90	12	28	55

produces task-specific scaling factors from this embedding. Let z_{task} denote the learned task embedding. We compute

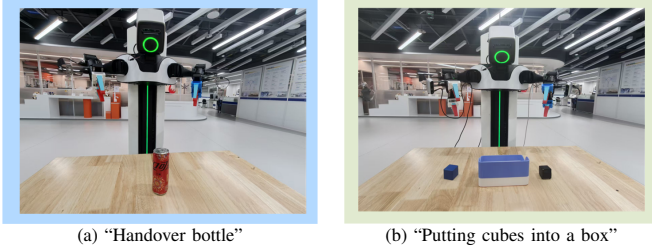


Fig. 4: Real-world task setup. (a) shows the dual-arm handover task, while (b) illustrates the task of putting cubes into a box.

scale (γ) and shift (β) parameters as follows:

$$[\gamma, \beta] = \text{MLP}_{FiLM}(z_{task}) \quad (5)$$

For the action query $Q \in \mathbb{R}^{k \times d_{model}}$, the modulated query Q' is formulated as:

$$Q' = \text{FiLM}(Q, z_{task}) = (1 + \gamma) \odot Q + \beta \quad (6)$$

This mechanism guarantees that the model’s behavior is strictly aligned with the specific task context throughout the execution.

2) *Multi-Scale Cross-Attention Layer*: Standard decoders attend only to the final encoder output, which can discard low-level visual details. We therefore introduce a multi-scale cross-attention mechanism. Each decoder layer d contains two cross-attention blocks:

$$\text{Out}_{inter} = \text{CA}(Q = Q', K = F_{low}, V = F_{low}) \quad (7)$$

$$\text{Out}_{final} = \text{CA}(Q = \text{Out}_{inter}, K = F_{enc}, V = F_{enc}) \quad (8)$$

where $\text{CA}(\cdot)$ denotes cross-attention. F_{enc} is the final output of the MoE encoder (high-level visual features), and F_{low} denotes intermediate features from the CNN backbone (ResNet-18) or lower encoder layers. This design provides rich and complementary visual information for action inference.

D. Training Objectives

The model is trained end-to-end to minimize a composite loss function \mathcal{L}_{total} :

$$\mathcal{L}_{total} = \mathcal{L}_{rec} + \lambda_{kl}\mathcal{L}_{kl} + \lambda_{MoE}\mathcal{L}_{MoE} \quad (9)$$

where \mathcal{L}_{rec} is the action reconstruction loss for imitation learning, \mathcal{L}_{kl} represents the Kullback-Leibler divergence loss for regularizing the CVAE latent space, and \mathcal{L}_{MoE} is the auxiliary loss for the MoE module. The coefficients λ_{kl} and λ_{MoE} are hyperparameters that weigh the contribution of the regularization and auxiliary terms, respectively.

1) *CVAE Loss*: Following the ACT policy framework, we employ the L1 norm for action reconstruction and the KL divergence to align the posterior distribution of the latent variable with the prior. The specific formulations are:

$$\begin{aligned} \mathcal{L}_{rec} &= \sum_t \|\hat{\mathbf{a}}_t - \mathbf{a}_t\|_1 \\ \mathcal{L}_{kl} &= D_{KL}(q(z|\mathcal{O}_t, \mathbf{a}_{t:t+k})\|p(z)) \end{aligned} \quad (10)$$

TABLE II: Ablation results for key components of MoE-ACT

Methods	Bottle	H/O	Pot	Fries	Skillet	Cab.	Avg.
w/o FiLM	24	64	60	82	16	32	46
w/o Multi-Scale Cross-Attention	40	68	64	74	10	28	47
Full Version	52	70	76	90	12	28	55

TABLE III: Real-world experimental comparison for multi-task bimanual manipulation

Methods	Handover Bottle	Putting Cubes into a Box	Avg.
ACT [2]	44	26	35
BAKU [24]	57	37	47
MoE-ACT (ours)	68	52	60

2) *MoE Auxiliary Loss*: To prevent mode collapse and ensure expert diversity, we introduce three auxiliary losses for the MoE module:

$$\mathcal{L}_{MoE} = -\alpha\mathcal{L}_{entropy} + \beta\mathcal{L}_{balance} + \gamma\mathcal{L}_{ortho} \quad (11)$$

- **Entropy Loss** ($\mathcal{L}_{entropy}$): Maximizes the entropy of the routing distribution to encourage the exploration of all experts.
- **Load Balancing Loss** ($\mathcal{L}_{balance}$): Penalizes the variance in expert assignment frequency to ensure an equal computational load across experts.
- **Orthogonal Loss** (\mathcal{L}_{ortho}): Minimizes the cosine similarity between expert weight matrices, encouraging experts to learn distinct features.

IV. EXPERIMENTAL RESULTS AND ANALYSIS

To evaluate the proposed method, we conduct multi-task learning experiments on the RoboTwin 2.0 benchmark [35] and in real-world settings. This section includes three parts: (1) comparison between MoE-ACT and representative baselines; (2) ablation studies on key architectural components; and (3) bimanual manipulation experiments on a physical robot to validate real-world multi-task performance.

A. Simulation Results

1) *Environmental Setup and Baselines*: In the multi-task setting, a unified policy is jointly trained on six representative bimanual manipulation tasks and evaluates that single policy on each task. MoE-ACT is trained with the Adam optimizer for 4000 epochs, using an initial learning rate of 1×10^{-5} and a batch size of 8. Training is performed on NVIDIA A800 GPUs. The training set contains 300 episodes in total, with 50 episodes per simulation task. We use Diffusion Policy (DP) [1], Action Chunking Transformer policy (ACT) [2], Robotics Diffusion Transformer (RDT) [12] for bimanual manipulation, and Transformer-based multi-task policy BAKU [24] as baselines. MoE-DP [33] is excluded from our comparison since its source code is not publicly available. Due to configuration issue, we report RDT scores excerpted from literature. All other baselines are independently evaluated by

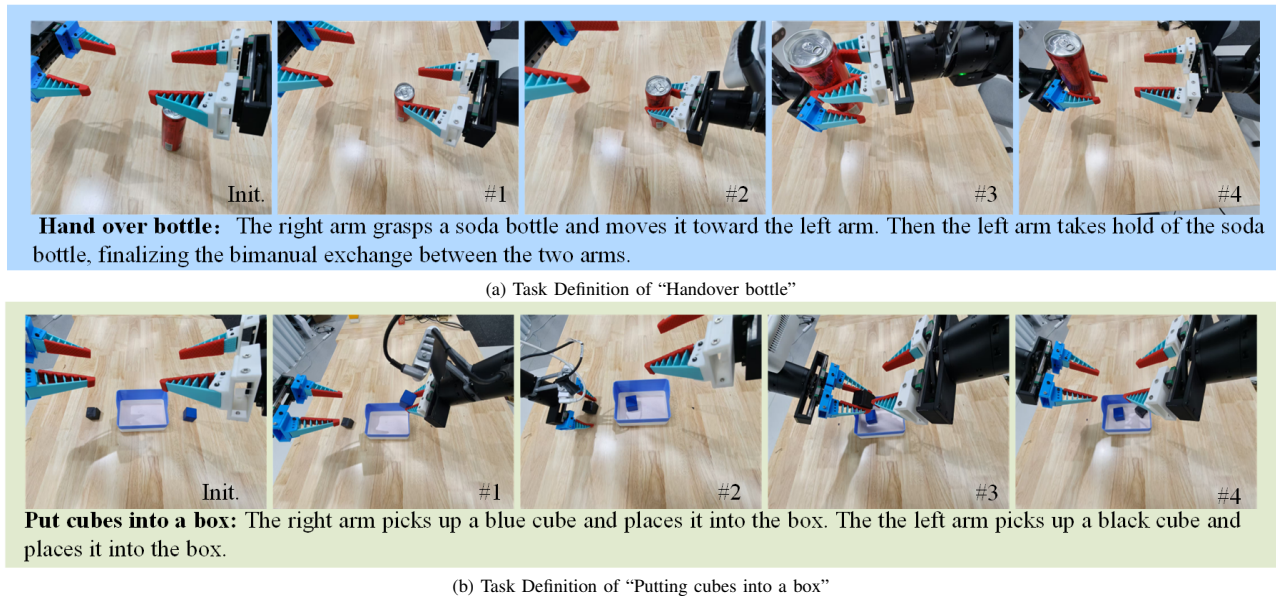


Fig. 5: Real-world task definitions. (a) shows the "Putting cubes into a box" task, which requires the robot to pick up cubes and place them into a box. (b) shows the "Handover bottle" task, where the robot must grasp a bottle and hand it to a human. These tasks evaluate the multi-task learning capability of MoE-ACT in real-world bimanual manipulation scenarios.

us. The hyperparameters and training settings follow their original implementations. For evaluation, we conduct 50 trials per task and reported the average success rates.

2) *Performance and Baseline Comparison:* As shown in Table I, ACT and DP perform poorly in this setting, likely due to the high degrees of freedom in dual-arm manipulation and multimodal action distributions in multi-task learning. Their average success rates across six tasks are 22% and 19%, respectively. RDT achieves 49% by scaling model parameters, but this gain comes at the cost of inference speed. By introducing MoE layers into the Transformer encoder, MoE-ACT learns multi-task action distributions more effectively and reaches an average success rate of 55% in simulation, outperforming ACT by 33%, RDT by 6%, and BAKU by approximately 24%. These results demonstrate the robustness and generalization capability of the proposed framework in complex environments.

Qualitatively, Fig. 2 visualizes expert activation during inference. For different tasks, MoE-ACT activates distinct experts based on the observation and task objective. The substantial variation in expert-weight distributions across tasks indicates meaningful specialization and diversity among experts.

B. Ablation Study

To quantify the contribution of each architectural component, we perform ablations by removing specific modules from the full MoE-ACT model. We compare the following variants: (1) Full Version (MoE-ACT): Contains both the FiLM conditioning and the Dual Cross-Attention mechanism. (2) w/o FiLM: Removes the task conditioning of FiLM. The task embedding is only injected via the input token sequence,

without modulating the action queries in the decoder layers. (3) w/o Multi-Scale Cross-Attention: Removes the additional cross-attention block over low-level visual features, while retaining the standard cross-attention block over final encoder features.

1) *Effect of FiLM Conditioning:* As shown in Table II, removing FiLM ("w/o FiLM") reduces average success rate by 9%. The decline is particularly pronounced on "Pick bottles", which is a 26% drop for that task. The performance gap demonstrates that language instruction can specify task objectives. FiLM-based conditioning helps the model adapt action inference to task-specific goals, thereby improving multi-task robotic learning.

2) *Effect of Multi-Scale Cross-Attention:* To intuitively demonstrate that the visual features extracted from different layers of the Transformer encoder capture distinct semantic properties, we visualize the cross-attention scores between the progressive decoder layers (Decoder L1-L5) and the multi-scale visual features. These attention heatmaps are obtained by extracting the cross-attention weights from the Transformer decoder during model inference. Specifically, the raw attention matrices are averaged across all action query tokens and attention heads to capture the model's overall spatial focus. Finally, the 1D attention weights are reshaped into 2D spatial grids and upsampled via bicubic interpolation. These grids are then overlaid onto the original RGB observations, with higher values represented by brighter colors.

As shown in Fig. 3, decoder attention differs substantially when querying low-level versus final-level visual features. When using low-level features (e.g., ResNet-18 and Encoder L1 outputs), attention is broader and captures global scene

context. When using final-level features, attention becomes spatially concentrated on the robot arms and target objects. Quantitatively, removing multi-scale cross-attention (“w/o Multi-Scale Cross-Attention”) reduces the average success rate by 8%. This result indicates that low-level visual features provide complementary information that improves scene understanding and task execution.

C. Real-World Experimental Results

1) *Experimental Setup*: The real-world multi-task experiments are conducted on the AIRBOT MMK2 platform using two bimanual tasks: “Handover bottle” and “Put cubes into a box.” As shown in Fig. 4, the robot is equipped with three Intel RealSense D435i cameras (one head-mounted and two wrist-mounted), providing rich and complementary visual feedback for bimanual manipulation. The robot uses 3D-printed TPU grippers. We collect 100 teleoperated trajectories (50 per task). For each method, a multi-task policy is trained, and performance is reported as the average success rate over 30 trials per task. All model inference is performed on an RTX 3050 GPU.

2) *Real Robot Bimanual Manipulation Performance*: As shown in Fig. 5, both tasks require coordinated bimanual control. Across tasks, MoE-ACT achieves the highest success rate, with a 60% average, corresponding to improvements of 25% and 13% over ACT and BAKU, respectively. For the “Handover bottle” task, MoE-ACT achieves a 68% success rate, outperforming ACT by 24% and BAKU by 11%. On “Putting cubes into a box” task, MoE-ACT improves success rate from 26% (ACT) to 52%, corresponding to a 100% relative gain.

3) *Failure Analysis*: It is worth noting that the success rate of “Putting Cubes into a Box” remains relatively modest. Most failures occur during grasping due to the small cube size. We also observe frequent failures when initial object positions are significantly shifted. A likely reason is the limited dataset size and insufficient diversity in object placements, which restrict robustness to complex scene variation. As a result, inference performance degrades under large shifts in initial placement. Future work aims to expand data diversity and apply data augmentation to improve generalization across initial configurations.

V. CONCLUSION

This paper presents MoE-ACT, a framework for multi-task learning for dual-arm robots. By integrating sparse MoE modules into the Transformer encoder, we effectively address performance challenges in multi-task robotic manipulation. Experimental results show that MoE-ACT outperforms ACT by approximately 33% in average success rate of multi-task manipulation on RoboTwin 2.0. It also demonstrates strong performance and robustness in real-world bimanual tasks. Although this study validates the potential of MoE for task decomposition, model scale and the number of experts can be further expanded. At present, optimal architectures and hyperparameters still require empirical tuning. Future work

will investigate larger-scale models for more general-purpose manipulation and unsupervised skill discovery within the MoE routing space.

REFERENCES

- [1] C. Chi, Z. Xu, S. Feng, E. Cousineau, Y. Du, B. Burchfiel, R. Tedrake, and S. Song, “Diffusion policy: Visuomotor policy learning via action diffusion,” *The International Journal of Robotics Research*, vol. 44, no. 10-11, pp. 1684–1704, 2025.
- [2] T. Z. Zhao, V. Kumar, S. Levine, and C. Finn, “Learning fine-grained bimanual manipulation with low-cost hardware,” *arXiv preprint arXiv:2304.13705*, 2023.
- [3] Y. Pu, Y. Niu, J. Tang, J. Xiong, S. Hu, and H. Li, “One model for all tasks: Leveraging efficient world models in multi-task planning,” *arXiv preprint arXiv:2509.07945*, 2025.
- [4] H. Liu, Y. Xue, Y. Zhou, H. Deng, Y. Liang, L. Xie, and Z. Wang, “Unimanip: General-purpose zero-shot robotic manipulation with agentic operational graph,” *arXiv preprint arXiv:2602.13086*, 2026.
- [5] J. Wen, Y. Zhu, J. Li, Z. Tang, C. Shen, and F. Feng, “Dexvla: Vision-language model with plug-in diffusion expert for general robot control,” *arXiv preprint arXiv:2502.05855*, 2025.
- [6] A. Prasad, K. Lin, J. Wu, L. Zhou, and J. Bohg, “Consistency policy: Accelerated visuomotor policies via consistency distillation,” *arXiv preprint arXiv:2405.07503*, 2024.
- [7] K. Bousmalis, G. Vezzani, D. Rao, C. Devin, A. X. Lee, M. Bauza, T. Davchev, Y. Zhou, A. Gupta, A. Raju *et al.*, “Robocat: A self-improving foundation agent for robotic manipulation,” *arXiv preprint arXiv:2306.11706*, vol. 1, no. 8, 2023.
- [8] K. Wu, Y. Zhu, J. Li, J. Wen, N. Liu, Z. Xu, and J. Tang, “Discrete policy: Learning disentangled action space for multi-task robotic manipulation,” in *2025 IEEE International Conference on Robotics and Automation (ICRA)*. IEEE, 2025, pp. 8811–8818.
- [9] B. Zitkovich, T. Yu, S. Xu, P. Xu, T. Xiao, F. Xia, J. Wu, P. Wohlhart, S. Welker, A. Wahid *et al.*, “Rt-2: Vision-language-action models transfer web knowledge to robotic control,” in *Conference on Robot Learning*. PMLR, 2023, pp. 2165–2183.
- [10] M. J. Kim, K. Pertsch, S. Karamcheti, T. Xiao, A. Balakrishna, S. Nair, R. Rafailov, E. Foster, G. Lam, P. Sanketi *et al.*, “Openvla: An open-source vision-language-action model,” *arXiv preprint arXiv:2406.09246*, 2024.
- [11] K. Black, N. Brown, D. Driess, A. Esmail, M. Equi, C. Finn, N. Fusai, L. Groom, K. Hausman, B. Ichter *et al.*, “ π_0 : A vision-language-action flow model for general robot control,” *arXiv preprint arXiv:2410.24164*, 2024.
- [12] S. Liu, L. Wu, B. Li, H. Tan, H. Chen, Z. Wang, K. Xu, H. Su, and J. Zhu, “RDT-1B: a diffusion foundation model for bimanual manipulation,” *arXiv preprint arXiv:2410.07864*, 2024.
- [13] K. Mei, Z. Tu, M. Delbraccio, H. Talebi, V. M. Patel, and P. Milanfar, “Bigger is not always better: Scaling properties of latent diffusion models,” *Transactions on Machine Learning Research*, 2024.
- [14] W. Cai, J. Jiang, F. Wang, J. Tang, S. Kim, and J. Huang, “A survey on mixture of experts in large language models,” *IEEE Transactions on Knowledge and Data Engineering*, 2025.
- [15] N. Shazeer, A. Mirhoseini, K. Maziarz, A. Davis, Q. Le, G. Hinton, and J. Dean, “Outrageously large neural networks: The sparsely-gated mixture-of-experts layer,” *arXiv preprint arXiv:1701.06538*, 2017.
- [16] D. Dai, C. Deng, C. Zhao, R. Xu, H. Gao, D. Chen, J. Li, W. Zeng, X. Yu, Y. Wu *et al.*, “Deepseekmoe: Towards ultimate expert specialization in mixture-of-experts language models,” in *Proceedings of the 62nd Annual Meeting of the Association for Computational Linguistics (Volume 1: Long Papers)*, 2024, pp. 1280–1297.
- [17] B. Hui, J. Yang, Z. Cui, J. Yang, D. Liu, L. Zhang, T. Liu, J. Zhang, B. Yu, K. Lu *et al.*, “Qwen2. 5-coder technical report,” *arXiv preprint arXiv:2409.12186*, 2024.
- [18] S. Huang, Z. Zhang, T. Liang, Y. Xu, Z. Kou, C. Lu, G. Xu, Z. Xue, and H. Xu, “Mentor: Mixture-of-experts network with task-oriented perturbation for visual reinforcement learning,” *arXiv preprint arXiv:2410.14972*, 2024.
- [19] R. Huang, S. Zhu, Y. Du, and H. Zhao, “Moe-loco: Mixture of experts for multitask locomotion,” in *2025 IEEE/RSJ International Conference on Intelligent Robots and Systems (IROS)*. IEEE, 2025, pp. 14 218–14 225.

- [20] C. Hao, X. Zhai, Y. Liu, and H. Soh, "Abstracting robot manipulation skills via mixture-of-experts diffusion policies," *arXiv preprint arXiv:2601.21251*, 2026.
- [21] Z. Li, A. Chapin, E. Xiang, R. Yang, B. Machado, N. Lei, E. Dellandrea, D. Huang, and L. Chen, "Robotic manipulation via imitation learning: Taxonomy, evolution, benchmark, and challenges," *arXiv preprint arXiv:2508.17449*, 2025.
- [22] B. Fang, S. Jia, D. Guo, M. Xu, S. Wen, and F. Sun, "Survey of imitation learning for robotic manipulation: B. fang et al." *International Journal of Intelligent Robotics and Applications*, vol. 3, no. 4, pp. 362–369, 2019.
- [23] H. Bharadhwaj, J. Vakil, M. Sharma, A. Gupta, S. Tulsiani, and V. Kumar, "Roboagent: Generalization and efficiency in robot manipulation via semantic augmentations and action chunking," in *2024 IEEE International Conference on Robotics and Automation (ICRA)*. IEEE, 2024, pp. 4788–4795.
- [24] S. Haldar, Z. Peng, and L. Pinto, "Baku: An efficient transformer for multi-task policy learning," *Advances in Neural Information Processing Systems*, vol. 37, pp. 141 208–141 239, 2024.
- [25] R. Shao, W. Li, L. Zhang, R. Zhang, Z. Liu, R. Chen, and L. Nie, "Large vlm-based vision-language-action models for robotic manipulation: A survey," *arXiv preprint arXiv:2508.13073*, 2025.
- [26] Y. Wang, P. Ding, L. Li, C. Cui, Z. Ge, X. Tong, W. Song, H. Zhao, W. Zhao, P. Hou *et al.*, "Vla-adapter: An effective paradigm for tiny-scale vision-language-action model," *arXiv preprint arXiv:2509.09372*, 2025.
- [27] A. O'Neill, A. Rehman, A. Maddukuri, A. Gupta, A. Padalkar, A. Lee, A. Pooley, A. Gupta, A. Mandlekar, A. Jain *et al.*, "Open x-embodiment: Robotic learning datasets and rt-x models: Open x-embodiment Collaboration⁰," in *2024 IEEE International Conference on Robotics and Automation (ICRA)*. IEEE, 2024, pp. 6892–6903.
- [28] A. Khazatsky, K. Pertsch, S. Nair, A. Balakrishna, S. Dasari, S. Karamcheti, S. Nasiriany, M. K. Srirama, L. Y. Chen, K. Ellis *et al.*, "DROID: A large-scale in-the-wild robot manipulation dataset," *arXiv preprint arXiv:2403.12945*, 2024.
- [29] A. Mandlekar, D. Xu, J. Wong, S. Nasiriany, C. Wang, R. Kulkarni, L. Fei-Fei, S. Savarese, Y. Zhu, and R. Martín-Martín, "What matters in learning from offline human demonstrations for robot manipulation," *arXiv preprint arXiv:2108.03298*, 2021.
- [30] A. Brohan, N. Brown, J. Carbajal, Y. Chebotar, J. Dabis, C. Finn, K. Gopalakrishnan, K. Hausman, A. Herzog, J. Hsu *et al.*, "Rt-1: Robotics transformer for real-world control at scale," *arXiv preprint arXiv:2212.06817*, 2022.
- [31] Z. Liang, Y. Mu, H. Ma, M. Tomizuka, M. Ding, and P. Luo, "Skilldiffuser: Interpretable hierarchical planning via skill abstractions in diffusion-based task execution," in *Proceedings of the IEEE/CVF Conference on Computer Vision and Pattern Recognition*, 2024, pp. 16 467–16 476.
- [32] J. Yang, H. Zhu, Y. Wang, G. Wu, T. He, and L. Wang, "Tra-moe: Learning trajectory prediction model from multiple domains for adaptive policy conditioning," in *Proceedings of the IEEE/CVF Conference on Computer Vision and Pattern Recognition*, 2025, pp. 6960–6970.
- [33] B. Cheng, T. Liang, S. Huang, M. Shao, F. Zhang, B. Xu, Z. Xue, and H. Xu, "Moe-dp: An moe-enhanced diffusion policy for robust long-horizon robotic manipulation with skill decomposition and failure recovery," *arXiv preprint arXiv:2511.05007*, 2025.
- [34] M. Reuss, J. Pari, P. Agrawal, and R. Lioutikov, "Efficient diffusion transformer policies with mixture of expert denoisers for multitask learning," *arXiv preprint arXiv:2412.12953*, 2024.
- [35] T. Chen, Z. Chen, B. Chen, Z. Cai, Y. Liu, Z. Li, Q. Liang, X. Lin, Y. Ge, Z. Gu *et al.*, "Robotwin 2.0: A scalable data generator and benchmark with strong domain randomization for robust bimanual robotic manipulation," *arXiv preprint arXiv:2506.18088*, 2025.